Solid State Nuclear Magnetic Resonance 87 (2017) 80–85

Contents lists available at ScienceDirect

Solid State Nuclear Magnetic Resonance

journal homepage: www.elsevier.com/locate/ssnmr

Hydrogen bond strength in membrane proteins probed by time-resolved ^{1}H-detected solid-state NMR and MD simulations

João Medeiros-Silva, Shehrazade Jekhmane, Marc Baldus, Markus Weingarth *

NMR Spectroscopy, Bijvoet Center for Biomolecular Research, Department of Chemistry, Utrecht University, Padualaan 8, 3584 CH Utrecht, The Netherlands

A B S T R A C T

^{1}H-detected solid-state NMR in combination with ^{1}H/^{2}D exchange steps allows for the direct identification of very strong hydrogen bonds in membrane proteins. On the example of the membrane-embedded potassium channel KcsA, we quantify the longevity of such very strong hydrogen bonds by combining time-resolved ^{1}H-detected solid-state NMR experiments and molecular dynamics simulations. In particular, we show that the carboxyl-side chain of the highly conserved residue Glu51 is involved in ultra-strong hydrogen bonds, which are fully-water-exposed and yet stable for weeks. The astonishing stability of these hydrogen bonds is important for the structural integrity of potassium channels, which we further corroborate by computational studies.

1. Introduction

The measurement of hydrogen-deuterium (^{1}H/^{2}D) exchange is a widespread method in solution NMR to probe protein structure [1], folding [2], and protein-ligand interactions [3]. Its principle is straightforward and based on the signal attenuation of exchangeable protons such as amino or hydroxyl protons upon incubation with deuterated solvents. How fast these protons exchange is usually determined by their participation in hydrogen bonds and by their surface exposure. The latter aspect renders ^{1}H/^{2}D exchange naturally a very attractive method to study membrane protein topology, which has been exploited in a number of solution NMR studies in micelles or detergents [4]. In solid-state NMR (ssNMR), however, ^{1}H/^{2}D exchange could not be directly exploited due a lack of ^{1}H-resolution. While the indirect ^{15}N-detection of ^{1}H/^{2}D exchange could already be used for elegant ssNMR studies on the topology of 7TM membrane proteins [5], we are likely to see many more applications of the simple ^{1}H/^{2}D exchange tool with the advent of high-resolution ^{1}H-detected ssNMR [6], driven by fast magic angle spinning (MAS). Indeed, we have recently used ^{1}H-detected ^{1}H/^{2}D exchange at fast MAS for the study of the membrane topology and the localization of functionally important water molecules in the ion channel KcsA [7]. Furthermore, ^{1}H-detected ^{1}H/^{2}D exchange ssNMR studies were conducted on the membrane protein proteorhodopsin [8] and on the SH3 domain [9].

Here we integrate time-resolved ^{1}H-detected ssNMR and molecular dynamics simulations to examine unusually strong hydrogen bonds in the membrane-embedded K^{+} channel KcsA. These hydrogen bonds are fully water-exposed and yet stable for many weeks, something that may hint at their potential functional importance.

2. Materials and methods

2.1. Sample preparation

Fractionally deuterated (FD) [7b] and inversely fractionally deuterated (iFD) [7c] ion channel KcsA were expressed and reconstituted as described previously. Importantly, FD [^{15}N,^{13}C]-KcsA was expressed in deuterated buffers, whereas iFD [^{15}N,^{13}C]-KcsA was expressed in protonated buffers. Therefore, only water-accessible amino-protons (H^{N}) are detectable in FD proteins, whereas also water-inaccessible H^{N} can be accessed in iFD proteins. ^{1}H/^{2}D exchange steps were performed with deuterated buffers (99.9% D_2O), in which the sample was incubated twice, and for one week in total, prior to the first measurement. Supplementary ^{1}H/^{2}D exchange steps were not necessary to back-protonate water-accessible parts of FD KcsA, because purification and reconstitution steps were performed in protonated buffers. All investigated ion channels were reconstituted with *E.coli* polar lipids in potassium phosphate buffer at pH 7 and were in the closed-conductive gating mode.

2.2. Solid-state NMR experiments

All experiments were performed at 21.1 T static magnetic field (800 MHz ^{1}H-frequency) and with 52 and 60 kHz MAS frequency for FD and iFD KcsA, respectively. The sample temperature was approximately

* Corresponding author.
E-mail address: m.h.weingarth@uu.nl (M. Weingarth).

https://doi.org/10.1016/j.ssnmr.2017.03.003
Received 30 December 2016; Received in revised form 9 March 2017; Accepted 13 March 2017
Available online 18 March 2017

303 K. ^{1}H-detected 2D NH spectra were acquired with a dipolar-based pulse sequence (described in Ref. [6e]) using MISSISSIPPI [10] solvent suppression. Low-power PISSARRO [11] decoupling (15 kHz decoupling power, pulse length ~70 μs) was applied in both the ^{15}N dimension and the ^{1}H dimension.

2.3. Molecular dynamics simulations

Atomistic MD simulations were run with the g53a6 force field [12] and the GROMACS package version 4.6.3 [13]. We used the X-ray structure 1K4C [14] embedded in anionic POPG lipids as starting system. Lipid parameters were obtained from Ref. [15]. The system contained the ion channel, 495 POPG lipids, 27914 water molecules, 513 K^+ and 30 Cl^- ions, adding up to 114460 atoms. The membrane insertion of the ion channel and further simulation parameters were handled as described previously [16]. The internuclear distances to analyze hydrogen bond stability were obtained with the *g_dist* tool of the GROMACS package. Distances were extracted in steps of 100 ps over a total simulation length of 300 ns.

3. Results and discussion

The membrane protein KcsA is an archetypical K^+ channel and a well-accepted model to study the gating of the central pore of K^+ channels [14,17]. We performed ^{1}H-detected studies of KcsA with the complementary labelling schemes *f*ractional *d*euteration (FD) and *i*nverse *f*ractional *d*euteration (iFD) (Fig. 1). These labelling schemes give access to exchangeable H^N only (FD in H_2O), all H^N (iFD in H_2O), and non-exchangeable H^N only (iFD in D_2O). Combining these labelling schemes represents hence a straightforward and powerful tool to study membrane protein topology. We could readily select residues that belong to the water-exposed outer vestibule (Fig. 1A) and the water-shielded transmembrane part (Fig. 1C) of KcsA. Note that the water-exposed cytoplasmic domain (CPD) is not visible in our dipolar-based spectra due to increased mobility, as we demonstrated previously [7b]. After incubating iFD KcsA in deuterated buffers for one week, almost all water-exposed residues of the outer vestibule fully exchanged, with the exceptions of V84H^N and T85H^N (Fig. 1C, highlighted in red bold letters). Astonishingly these residues did not exchange, in spite of the fact that they are fully accessible by the bulk water (Fig. 2). Note that T85 was also protected from exchange in native bacterial membranes (see Fig. 2E in Ref. [7c]).

This suggested that V84 and T85 are involved in exceptionally strong hydrogen bonds, which may relate to their localization at the water-membrane interface, which is a region of low dielectric permittivity (Fig. 2D). In the KcsA crystal structure (pdb 1K4C) [14], the backbone amino-protons of both V84 and T85 form hydrogen bonds with the carboxyl side chain of residue E51, connecting the TM1 helix with the pore-loop (P-loop). This hydrogen bond pattern is also present in other K^+ channels, such as in Shaker or the KCNKØ channel, which was demonstrated with cysteine-crosslinking [18]. Residue E51 (E418 in Shaker, E28 in KCNKØ) is conserved in most K^+ channels and absolutely

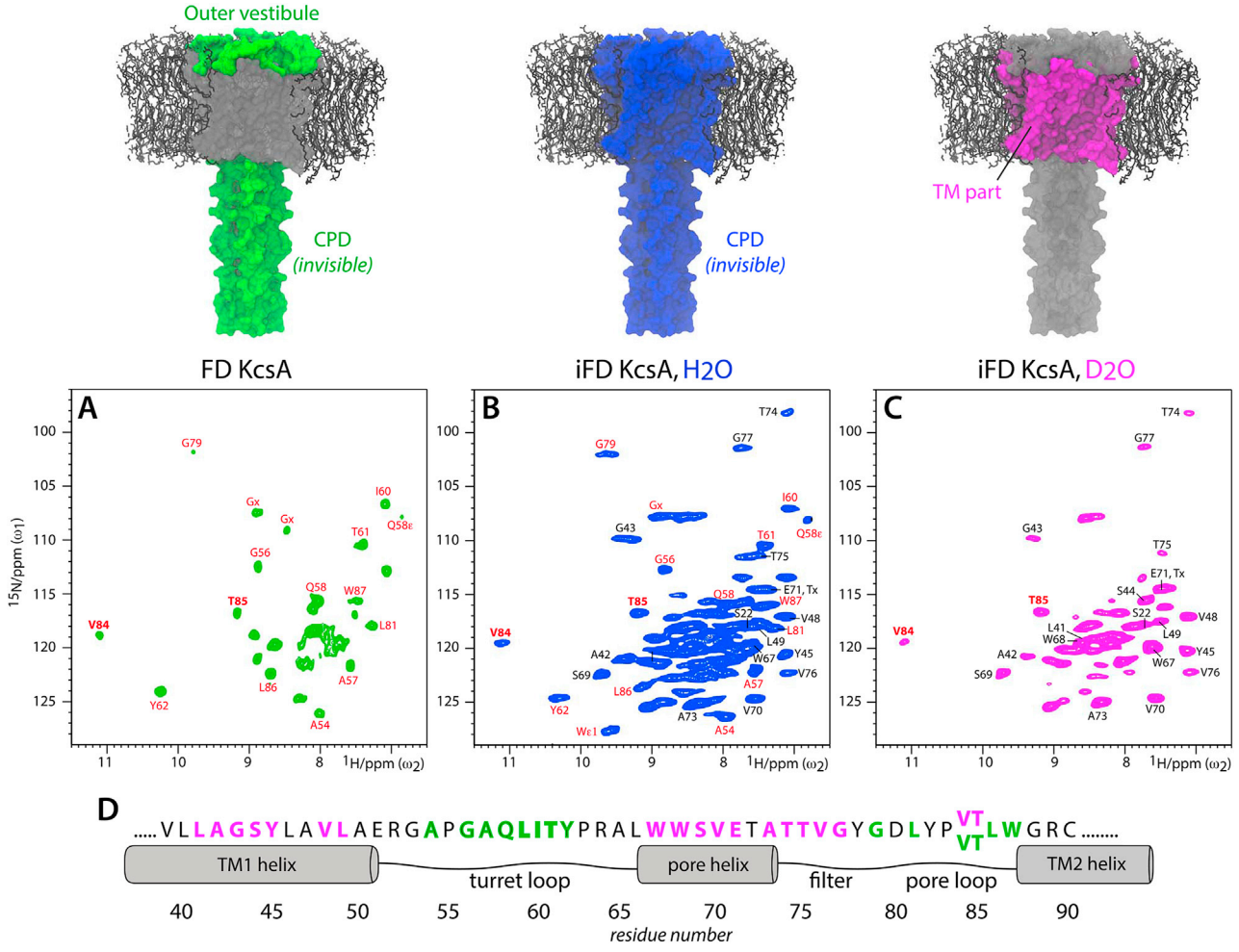

Fig. 1. ^{1}H-detected dipolar-based 2D NH spectra of A) FD KcsA, B) iFD KcsA in protonated buffers, and C) iFD KcsA in deuterated buffers. Spectra were acquired at 800 MHz and with 52 and 60 kHz MAS for FD and iFD KcsA, respectively. Signals of V84 and T85 are annotated in red bold letters. D) Illustration of visible H^N signals in FD KcsA (green) and D_2O-incubated iFD KcsA (magenta). Residues in black color are not assigned. (For interpretation of the references to color in this figure legend, the reader is referred to the web version of this article.)

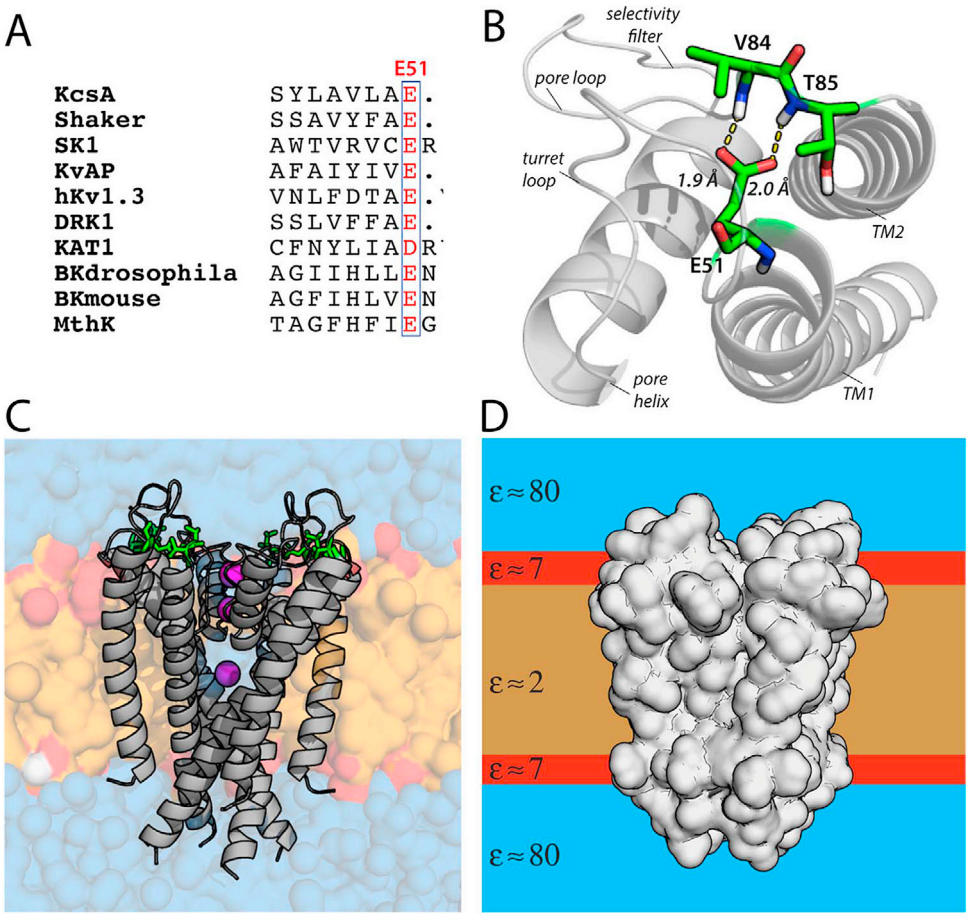

Fig. 2. A) Sequential alignment of several K^+ channels, showing the absolute conservation of E51 in voltage-gated K^+channels. B) Illustration of the V84/T85 – E51 hydrogen bond network in KcsA. C) E51 and V84/T85 (shown in green) are fully water exposed and localized at the water-lipid interface. D) Illustration of the profile of dielectric constants ε across lipid bilayers. The low permittivity at the membrane interface increases Coulomb contributions in hydrogen bonds. (For interpretation of the references to color in this figure legend, the reader is referred to the web version of this article.)

conserved in voltage-gated potassium (Kv) channels (Fig. 2A). Several studies have reported that residue E51 is important for slow C-type inactivation in Kv channels, which was demonstrated with mutational studies in Shaker, BK2, and the KCNKØ channel [18,19]. Furthermore, E51 seems relevant for structural integrity, given that certain E51X KcsA mutants failed to express [20], and E51 was shown to be a pH sensor in the TASK2 channel [21]. It seems hence plausible that the very strong hydrogen bonds formed by the E51 side chain relates to the importance of this residue.

To quantify the stability of the hydrogen bonds in which $V84H^N$ and $T85H^N$ are involved, we performed time-resolved ssNMR experiments. We measured additional ^{1}H-detected 2D NH spectra with iFD KcsA after four and seven weeks of incubation time in deuterated buffers (Fig. 3). To quantify the gradual signal decay of $V84H^N$ and $T85H^N$ due to $^1H/^2D$ exchange, we referenced to the water-shielded transmembrane residues V48 and V70, which are not affected by exchange. Our analysis revealed that $V84H^N$ exchanged substantially faster than $T85H^N$. Whereas the T85 signal had lost only about 10% intensity after 4 weeks of incubation time, the V84 signal was reduced by 60% in intensity. This suggested a significant difference in the hydrogen bond strength for these two residues. Such a marked difference is not deducible from the crystal structure 1K4C [14], in which the V84 – E51 hydrogen bond is actually even 0.1 Å shorter than the T85 – E51 hydrogen bond. We hence wondered if the decay differences observed by time-resolved ^{1}H-detected ssNMR really directly related to the differential longevity of the V84 – E51 and T85 – E51 hydrogen bonds.

To gain further insight in hydrogen bond stability, we performed atomistic molecular dynamics (MD) simulations. We used a closed-conductive KcsA structure (pdb 1K4C) embedded in anionic POPG lipids as starting system. Fig. 4A shows the temporal evolution of the distances between the V84/T85 amino-protons and the closer of the two E51 side chain carboxyl-oxygens, and this is the relevant hydrogen bond distance. The analysis was conducted over 300 ns of MD simulation (Fig. 4A,B). We could indeed observe a clear difference in hydrogen bond stability, which is perfectly in line with our time-resolved solid-state NMR data. The T85 hydrogen bond length is extremely steady, and does basically not exceed 2.5 Å over the evaluated period. This is most likely because the T85 hydroxyl side chain further stabilizes the hydrogen bond (Fig. 4C). However, for V84, we observe more than 200 times distances exceeding 2.5 Å, and we even observe a small but significant number of distances that exceed 3.5 Å. Distances around 3.5 Å mark a loss of hydrogen bonding during which $V84H^N$ is accessible to bulk water and can exchange (Fig. 4C, see also supporting video S1). In total, the loss of hydrogen bonding for $V84H^N$ occurred three times over the evaluated period of 300 ns. The MD simulations hence show that while both V84 and T85 form very tight hydrogen bonds with E51, the hydrogen bond with T85 is far stronger. Both observations agree remarkably well with our time-resolved ^{1}H-detected ssNMR data.

Supplementary material related to this article can be found online at https://doi.org/10.1016/j.ssnmr.2017.03.003.

Note that an analysis of H^N – water distances over the trajectory clearly demonstrated that $V84H^N$ and $T85H^N$ are refractory to exchange despite the steady presence of close water molecules (Fig. S1). We also like to emphasize that the strong V84/T85 signals in FD KcsA (Fig. 1A)

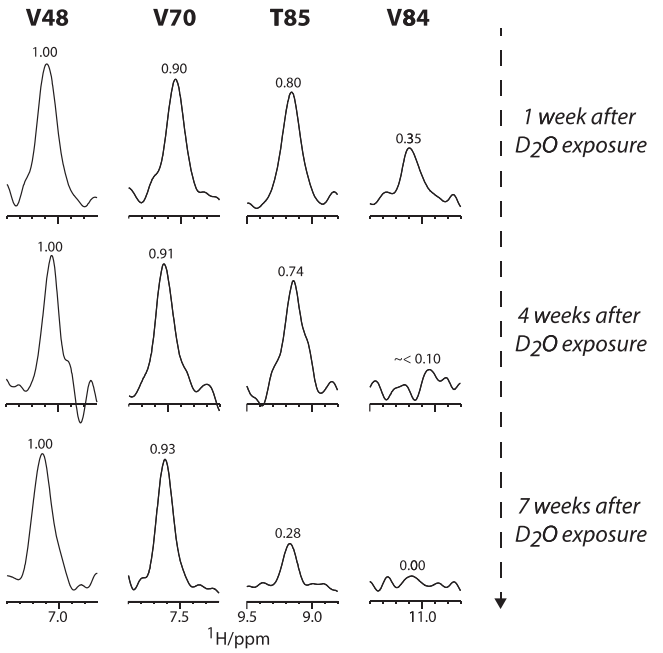

Fig. 3. The decay of signals V84 and T85 as a function of the incubation time in deuterated buffers. For each measurement point, we referenced the signal heights of V84/T85 to the transmembrane residues V48/V70. The latter are not prone to $^{1}H/^{2}H$ exchange. Note that the accelerated decay of T85 between 4 and 7 weeks of D_2O-exposure is presumably due to sample heating effects.

are not at all in contradiction to our conclusions. While FD KcsA is grown in deuterated buffers, purification and reconstitution steps, which take several days, are performed in protonated buffers. During these steps, signals of the water-accessible outer vestibule fully exchange. Moreover, in the absence of a bilayer, the outer vestibule is less densely packed (absence of bilayer lateral pressure) and the low permittivity environment of the bilayer (Fig. 2D) is absent.

The enormous stability of the V84/T85 – E51 hydrogen bonds is surprising. In voltage-gated and other K^{+} channels, it was shown that loss of interactions with E51 led to a stark acceleration of C-type inactivation [18,19]. In line with this notion, it was demonstrated that linking S5 with the S6-P-loop via E418 in Shaker (E51 in KcsA) greatly stabilizes the inactivation gate [18b]. It hence seems plausible that the hydrogen bonds formed by the E51 side chain are therefore tightly controlled. In atomistic MD simulations with a E51A KcsA mutant, we see that loss of the V84/T85 – E51 hydrogen bonds goes along with marked structural alterations in the turret loop (Fig. 5). The Baldus group [16b] and the Perozo group [22] have recently demonstrated that the turret region modulates KcsA gating, presumably via the selectivity filter. The detailed structural underpinning of the influence of the turret on gating is however yet elusive. However, that the structure or the dynamics of the outer vestibule is linked to channel gating appears obvious, given that specific lipid binding at the outer vestibule modulates channel gating by yet unknown mechanisms [16a,23]. Against this backdrop, it is tempting to speculate that the strong hydrogen bonds formed by E51 are a kind of trigger that, via the outer vestibule, act on the selectivity filter.

4. Conclusions

We have reported an approach based on time-resolved ^{1}H-detected ssNMR and MD simulations that allows quantifying very strong water-exposed hydrogen bonds. This is especially interesting, since such bonds are usually not readily identifiable in X-ray structures. Our approach allowed us to identify a network of outstandingly strong hydrogen bonds in the water-exposed turret loop of KcsA. Interestingly,

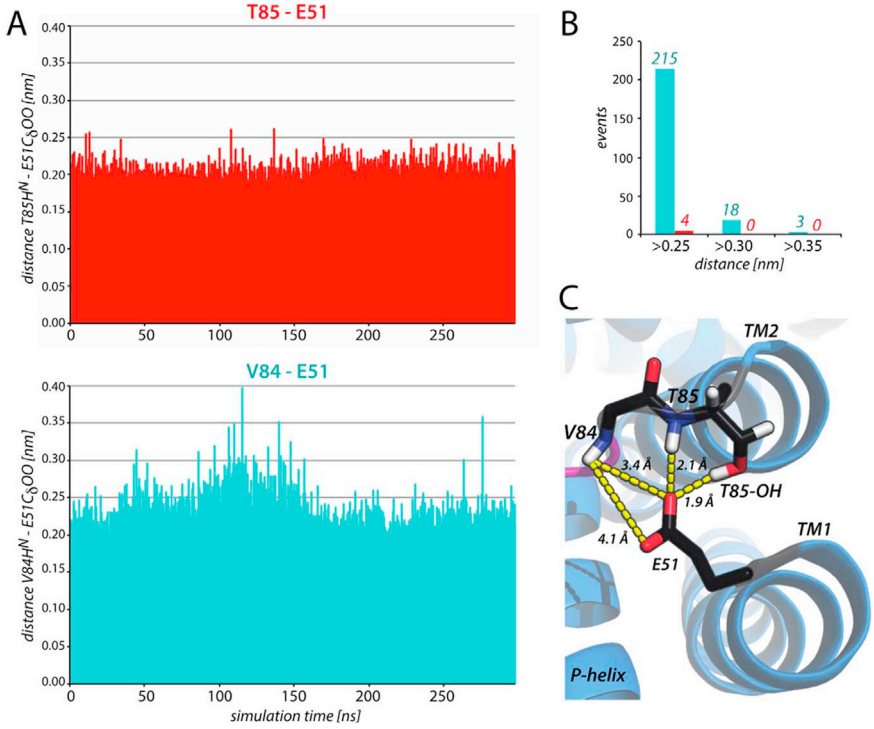

Fig. 4. Analysis of hydrogen bond stability from MD simulations. A) Temporal evolution of the distance between the V84/T85 amino-proton and the carboxyl-oxygen of E51. For each analysis step, the distance to the closer carboxyl oxygen is plotted. The analysis reflects the hydrogen bond distance in one monomer of the tetrameric KcsA channel. Similar pattern were found in the other three protomers. B) Summary of the distance evolution shown in A). Distances around 3.5 Å correspond to a loss of hydrogen bonding. C) Although a rare event, the V84 – E51 hydrogen bond breaks from time to time, which leaves $V84H^{N}$ prone to $^{1}H/^{2}D$ exchange. The T85 side chain hydroxyl-group further stabilizes the T85 – E51 hydrogen bond.

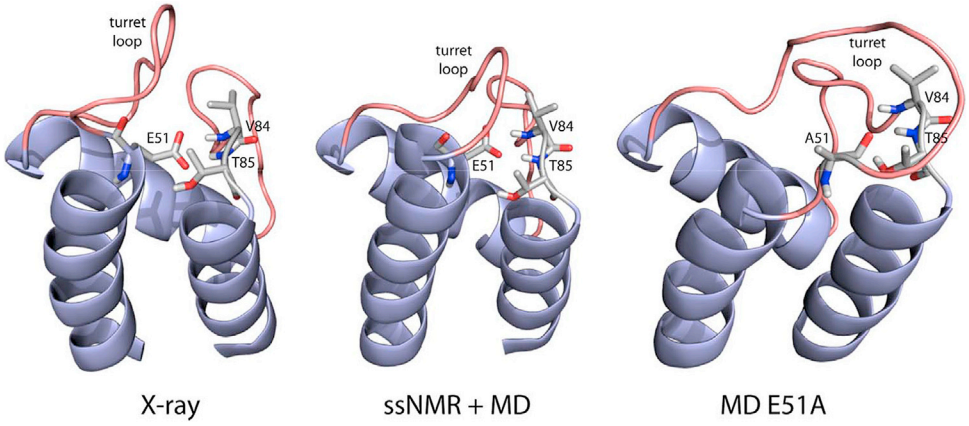

Fig. 5. KcsA structural alignment of (left) X-ray structure 1K4C, (middle) the ssNMR model [16b] from KcsA (after MD simulation), which shows an extended TM1 helix, and (right) the E51A mutant after 90 ns of MD simulations, showing a starkly different turret loop.

this network appears to be conserved in eukaryotic voltage-gated potassium (Kv) channels. We expect that this approach is amenable to a large number of proteins, especially to membrane proteins. Indeed, the unusual strength of the here-described hydrogen bonds likely relates to their location in the interfacial membrane region (Fig. 2D). The membrane interface is a zone of low dielectric permittivity (dielectric constant $\varepsilon \sim 7$, as compared to $\varepsilon \sim 80$ in bulk water), which strengthens the Coulomb interactions in hydrogen bonds. Since any membrane protein features residues at the membrane interface, such ultra-strong, water-exposed hydrogen bonds may be rather the rule than the exception, and may be of special structural or functional importance. Notably, it was recently reported in a ssNMR study that a number of residues in the interfacial loops of human aquaporin-1 were protected from $^{1}H/^{2}D$ exchange [24]. For future studies, it may be advantageous to use lower temperatures to slow down $^{1}H/^{2}D$ exchange, or to use shorter D_2O incubation times to distinguish more nuances of hydrogen bond strength.

Acknowledgement

We greatly acknowledge financial support by The Netherlands Organisation for Scientific Research (NWO) (grant numbers 723.014.003 and 700.10.443).

Appendix A. Supporting information

Supplementary data associated with this article can be found in the online version at https://doi.org/10.1016/j.ssnmr.2017.03.003.

References

[1] (a) G. Wagner, K. Wuthrich, J. Mol. Biol. 160 (1982) 343–361;
(b) M. Hoshino, H. Katou, Y. Hagihara, K. Hasegawa, H. Naiki, Y. Goto, Nat. Struct. Biol. 9 (2002) 332–336.
[2] (a) T. Raschle, P.R. Flores, C. Opitz, D.J. Muller, S. Hiller, Angew. Chem. Int Ed. 55 (2016) 5952–5955;
(b) S.W. Englander, L. Mayne, Annu. Rev. Biophys. Biomol. Struct. 21 (1992) 243–265.
[3] V.I. Polshakov, B. Birdsall, J. Feeney, J. Mol. Biol. 356 (2006) 886–903.
[4] (a) T.J. Pinheiro, H. Cheng, S.H. Seeholzer, H. Roder, J. Mol. Biol. 303 (2000) 617–626;
(b) O. Halskau, N.A. Froystein, A. Muga, A. Martinez, J. Mol. Biol. 321 (2002) 99–110;
(c) X. Yao, U.H.N. Durr, Z. Gattin, Y. Laukat, R.L. Narayanan, A.K. Bruckner, C. Meisinger, A. Lange, S. Becker, M. Zweckstetter, PLoS One 9 (2014).
[5] (a) L.C. Shi, I. Kawamura, K.H. Jung, L.S. Brown, V. Ladizhansky, Angew. Chem. Int. Ed. 50 (2011) 1302–1305;
(b) S.L. Wang, L.C. Shi, I. Kawamura, L.S. Brown, V. Ladizhansky, Biophys. J. 101 (2011) L23–L25.
[6] (a) Y. Ishii, R. Tycko, J. Magn. Reson. 142 (2000) 199–204;
(b) V. Chevelkov, K. Rehbein, A. Diehl, B. Reif, Angew. Chem. Int. Ed. 45 (2006) 3878–3881;
(c) D.H. Zhou, G. Shah, M. Cormos, C. Mullen, D. Sandoz, C.M. Rienstra, J. Am. Chem. Soc. 129 (2007) 11791–11801;
(d) V. Agarwal, S. Penzel, K. Szekely, R. Cadalbert, E. Testori, A. Oss, J. Past, A. Samoson, M. Ernst, A. Bockmann, B.H. Meier, Angew. Chem. Int. Ed. 53 (2014) 12253–12256;
(e) T. Sinnige, M. Daniels, M. Baldus, M. Weingarth, J. Am. Chem. Soc. 136 (2014) 4452–4455;
(f) V. Chevelkov, B. Habenstein, A. Loquet, K. Giller, S. Becker, A. Lange, J. Magn. Reson. 242 (2014) 180–188;
(g) J.M. Lamley, C. Oster, R.A. Stevens, J.R. Lewandowski, Angew. Chem. Int. Ed. Engl. 54 (2015) 15374–15378;
(h) P. Ma, Y. Xue, N. Coquelle, J.D. Haller, T. Yuwen, I. Ayala, O. Mikhailovskii, D. Willbold, J.P. Colletier, N.R. Skrynnikov, P. Schanda, Nat. Commun. 6 (2015) 8361;
(i) L.B. Andreas, K. Jaudzems, J. Stanek, D. Lalli, A. Bertarello, T. Le Marchand, D.C.D. Paepe, S. Kotelovica, I. Akopjana, B. Knott, S. Wegner, F. Engelke, A. Lesage, L. Emsley, K. Tars, T. Herrmann, G. Pintacuda, Proc. Natl. Acad. Sci. USA 113 (2016) 9187–9192.
[7] (a) M. Weingarth, E.A.W. van der Cruijsen, J. Ostmeyer, S. Lievestro, B. Roux, M. Baldus, J. Am. Chem. Soc. 136 (2014) 2000–2007;
(b) D. Mance, T. Sinnige, M. Kaplan, S. Narasimhan, M. Daniels, K. Houben, M. Baldus, M. Weingarth, Angew. Chem. Int. Ed. Engl. 54 (2015) 15799–15803;
(c) J. Medeiros-Silva, D. Mance, M. Daniels, S. Jekhmane, K. Houben, M. Baldus, M. Weingarth, Angew. Chem. Int. Ed. Engl. 55 (2016) 13606–13610.
[8] M.E. Ward, L. Shi, E. Lake, S. Krishnamurthy, H. Hutchins, L.S. Brown, V. Ladizhansky, J. Am. Chem. Soc. 133 (2011) 17434–17443.
[9] J.M. Lopez, del Amo, U. Fink, B. Reif, J. Biomol. NMR 48 (2010) 203–212.
[10] D.H. Zhou, C.M. Rienstra, J. Magn. Reson. 192 (2008) 167–172.
[11] (a) M. Weingarth, P. Tekely, G. Bodenhausen, Chem. Phys. Lett. 466 (2008) 247–251;
(b) M. Weingarth, G. Bodenhausen, P. Tekely, J. Magn. Reson. 199 (2009) 238–241;
(c) M. Weingarth, G. Bodenhausen, P. Tekely, Chem. Phys. Lett. 502 (2011) 259–265.
[12] T.A. Soares, P.H. Hunenberger, M.A. Kastenholz, V. Krautler, T. Lenz, R.D. Lins, C. Oostenbrink, W.F. Van Gunsteren, J. Comput. Chem. 26 (2005) 725–737.
[13] B. Hess, C. Kutzner, D. van der Spoel, E. Lindahl, J. Chem. Theory Comput. 4 (2008) 435–447.
[14] Y.F. Zhou, J.H. Morais-Cabral, A. Kaufman, R. MacKinnon, Nature 414 (2001) 43–48.
[15] A. Kukol, J. Chem. Theory Comput. 5 (2009) 615–626.
[16] (a) M. Weingarth, A. Prokofyev, E.A. van der Cruijsen, D. Nand, A.M. Bonvin, O. Pongs, M. Baldus, J. Am. Chem. Soc. 135 (2013) 3983–3988;
(b) E.A. van der Cruijsen, D. Nand, M. Weingarth, A. Prokofyev, S. Hornig, A.A. Cukkemane, A.M. Bonvin, S. Becker, R.E. Hulse, E. Perozo, O. Pongs, M. Baldus, Proc. Natl. Acad. Sci. USA 110 (2013) 13008–13013.
[17] (a) A. Lange, K. Giller, S. Hornig, M.F. Martin-Eauclaire, O. Pongs, S. Becker, M. Baldus, Nature 440 (2006) 959–962;
(b) C. Ader, R. Schneider, S. Hornig, P. Velisetty, E.M. Wilson, A. Lange, K. Giller, I. Ohmert, M.F. Martin-Eauclaire, D. Trauner, S. Becker, O. Pongs, M. Baldus, Nat. Struct. Mol. Biol. 15 (2008) 605–612;
(c) J.F. Cordero-Morales, L.G. Cuello, Y.X. Zhao, V. Jogini, D.M. Cortes, B. Roux, E. Perozo, Nat. Struct. Mol. Biol. 13 (2006) 311–318;
(d) C. Ader, R. Schneider, S. Hornig, P. Velisetty, V. Vardanyan, K. Giller, I. Ohmert, S. Becker, O. Pongs, M. Baldus, EMBO J. 28 (2009) 2825–2834.
[18] (a) N. Zilberberg, N. Ilan, S.A.N. Goldstein, Neuron 32 (2001) 635–648;
(b) H.P. Larsson, F. Elinder, Neuron 27 (2000) 573–583.
[19] P. Ortega-Saenz, R. Pardal, A. Castellano, J. Lopez-Barneo, J. Gen. Physiol. 116 (2000) 181–190.
[20] S. Imai, M. Osawa, K. Takeuchi, I. Shimada, Proc. Natl. Acad. Sci. USA 107 (2010) 6216–6221.

[21] M.J. Morton, A. Abohamed, A. Sivaprasadarao, M. Hunter, Proc. Natl. Acad. Sci. USA 102 (2005) 16102–16106.
[22] H. Raghuraman, S.M. Islam, S. Mukherjee, B. Roux, E. Perozo, Proc. Natl. Acad. Sci. USA 111 (2014) 1831–1836.
[23] (a) P. Marius, M.R.R. de Planque, P.T.F. Williamson, BBA-Biomembr. 1818 (2012) 90–96;
(b) E.A. van der Cruijsen, A.V. Prokofyev, O. Pongs, M. Baldus, Biophys. J. 112 (2017) 99–108;
(c) M. Weingarth, M. Baldus, Acc. Chem. Res. 46 (2013) 2037–2046.
[24] S.L. Wang, C. Ing, S. Emami, Y.J. Jiang, H.J. Liang, R. Pomes, L.S. Brown, V. Ladizhansky, J. Phys. Chem. B 120 (2016) 9887–9902.